PRELIMINARY MODEL FOR PERIOD-DEPENDENT DURATION

Norman Abrahamson and Chih-Hsuan Sung

Department of Civil & Environmental Engineering University of California, Berkeley

Abstract

A new period-dependent duration based on the cumulative-squared response of a 50%-damped single-degree-of-freedom oscillator is presented. For T>1 sec, the duration is systematically larger than the accelerogram-based duration. There is a large variability of the ratio of the long-period duration to the acceleration-based duration. To develop design time histories for structure sensitive to the long period ground motion, the long-period duration of the time histories should be considered in the selection process. A preliminary conditional ground-motion model for period-dependent duration is presented. A final updated period-dependent ground-motion model will be developed by the end of the project.

Introduction

The damage potential of strong ground motion is mainly characterized by the amplitude of shaking, but the duration of the shaking can also affect the damage potential of the ground motion for some structures. The importance of duration on structural performance depends on the type of structure and the damage measure used, leading to varying conclusions about the significance of duration on the damage to structures (Hancock and Boomer, 2006; Bommer et al., 2009). In addition to the dependence on the type of structure and damage measure, the varying conclusions about the importance of duration on structural response may also be related to the duration metric used. Bommer and Martínez-Pereira (1999) noted that over 30 different

Duration has two main uses in seismic hazard and ground motion studies. In seismic hazard studies, the main use of duration models is to set the expected duration for the design ground motions which is then used to guide the selection of ground-motion time series for later use in the dynamic analyses of the structure. In ground-motion studies, the duration models are used in the application of random vibration theory (RVT) to convert Fourier Amplitude Spectra (FAS) to response spectral values (Boore and Thompson, 2014).

Currently, the most widely used duration metric is based on the normalized Arias intensity, AI_N, (Arias, 1970):

$$AI_N(t) = \frac{\int_0^t a^2(\tau)d\tau}{\int_0^{tmax} a^2(\tau)d\tau}$$
 (1)

in which AI_N is the normalized Arias Intensity and $a(\tau)$ is the acceleration time series. Equation (1) can be inverted to give the time as a function of the AI_N . The significant duration is defined as the time between the AI_N reaches two selected percentages, X and Y:

$$D_{X-Y} = t(AI_N - Y) - t(AI_N - X)$$
 (2)

The $t(AI_N - X)$ is the time at which the normalized Arias intensity is equal to X. For example, the time between the AI reaching 5% of the total and 75% of the total is called the D₅₋₇₅ duration.

Multiple empirical models for the D₅₋₇₅ and D₅₋₉₅ duration based on the normalized AI have been developed over the years. Recent duration models, such as Afshari and Stewart (2016), Du and Wang (2017)} which are based on the NGA-W2 data set (Ancheta et al, 2014), are commonly used in California seismic hazard studies. These models give the duration for the D₅₋₇₅ and D₅₋₉₅. By using the acceleration time series to define duration for the design ground motion, there is an implicit assumption that acceleration duration represents the duration of the ground motion for the period of interest for the structure. That is, the assumption is that the ground-motion duration is the same for all periods. As shown below, this assumption does not hold for long-period ground motion (T>1 sec). In this paper, we propose a period-dependent duration metric that can be used to develop a duration spectrum to complement the response spectrum.

Period-Dependent Duration

One approach to the period dependence of duration is to develop duration models for velocity and displacement time series, analogous to the current approach used for acceleration by simply substituting the velocity or displacement time series for the acceleration time series in equation (2). As an example, the acceleration, velocity, and displacement time series for the Sunland - Mt Gleason Ave recording of the 1994 Northridge earthquake (M=6.7, R_{RUP}=13 km, V_{S30}=446 m/s) is shown in Figure 1. For this recording, the D₅₋₇₅ duration values for the velocity and displacement time series are longer than for the acceleration time series. The drawback of this approach is the predominate period for velocity depends on magnitude: the predominate periods of velocity and displacement are longer for larger magnitude earthquakes. As a result, the duration for velocity for moderate-magnitude earthquakes will sample a different period range than for large-magnitude earthquakes, making it more difficult to develop a simple empirical model that captures the period dependence of the duration using velocity time series.

To directly address the period dependence of duration, we use the cumulative-squared acceleration of the response of a high-damped (50% damping) single-degree of freedom (SDOF) oscillator. That is, we replace the acceleration time series with the time series of the 50%-damped SDOF response. A large damping value is used so that the duration of the response of the SDOF represents the duration of the input ground motion and is less affected by the elongated duration due to the oscillator response. For a spectral period of T=0 sec, the SDOF response is equal to the acceleration time series, so the duration for T=0 will be the same as the current duration metric based on the AI_N. A related period-dependent intensity measure was proposed by Travasarou (2003) in which the period-dependent Arias intensity was computed

from the SDOF response at 5% damping. The main difference between these two metrics is that we use a much larger damping, and we use the normalized Arias intensity.

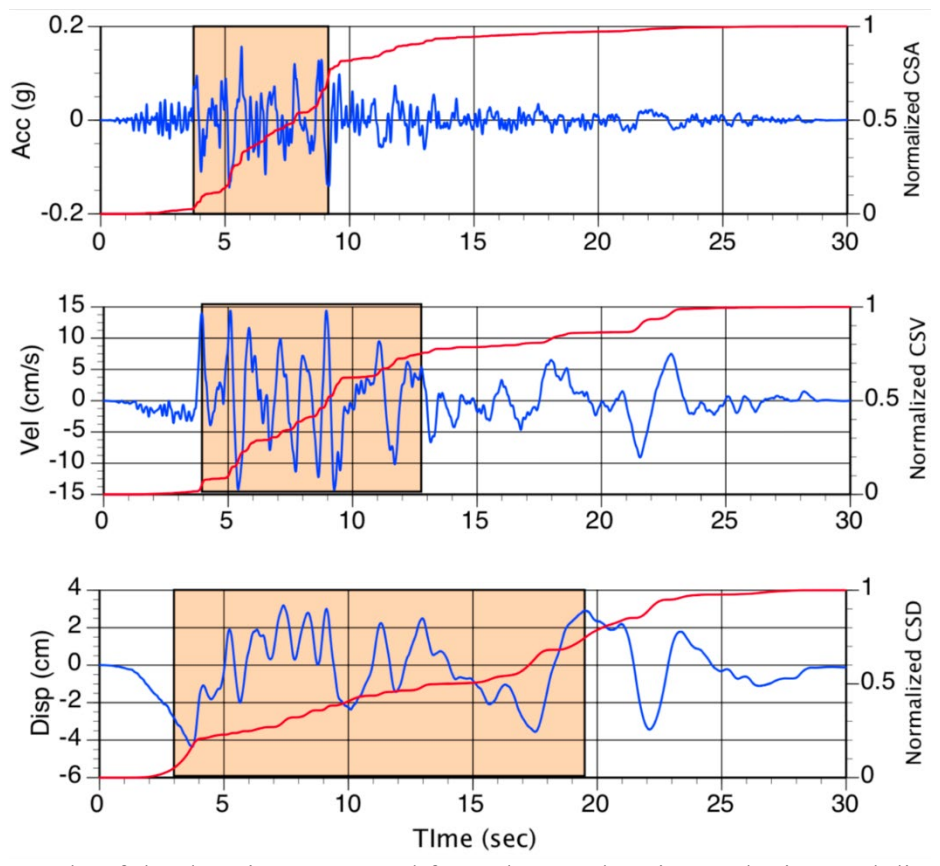


Figure 1. Example of the duration measured from the acceleration, velocity, and displacement time series.

Using the same Sunland recording from the Northridge earthquake, the time series of the response of a 50%-damped SDOF oscillator is shown in Figure 2 for five spectral periods. Similar to the increase in duration for the velocity and displacement time series shown in Figure 1, there is an increase in the duration for the two longer periods for this recording. Computing the duration of the high-damped oscillator for a range of spectral periods, we develop the period dependence of the D_{5-75} shown in Figure 3. This represents a duration spectrum.

For this recording, the D_{5-75} duration is nearly constant for periods up to 1 sec and then increases rapidly: the D_{5-75} duration increases from about 5 sec at short periods to 16-18 sec at long periods (T=2 to T=7 sec), likely due to trapped basin waves in the San Fernando basin. This increase in the duration at long periods is not seen for all recordings. For example, the duration spectra for two recordings from the Northridge earthquake with similar rupture distances of about 15 km are shown in Figure 3. These two recordings have similar D_{5-75} duration values for the traditional acceleration-based duration (i.e., the period-dependent duration for T=0 sec), but they have very different D_{5-75} duration values for long periods. This highlights a key limitation of using only the duration based on the AI for selecting time histories for dynamic analyses of structures: if the target D_{5-75} duration was 5-6 sec, both of these recordings would satisfy the

duration for the AI, but they may lead to very different responses for geotechnical system with a natural period of 2 sec or more (such as large tailings dams) or for building response if the building has a long natural period and the structural response measure is duration sensitive.

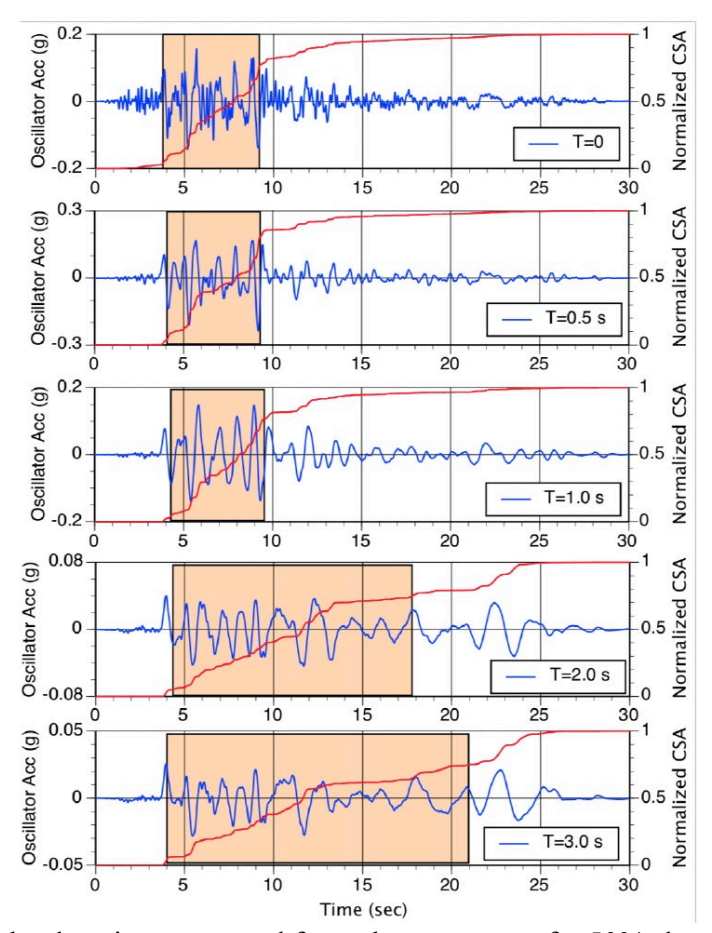


Figure 2. Example of the duration measured from the response of a 50%-damped SDOF for a range of oscillator periods.

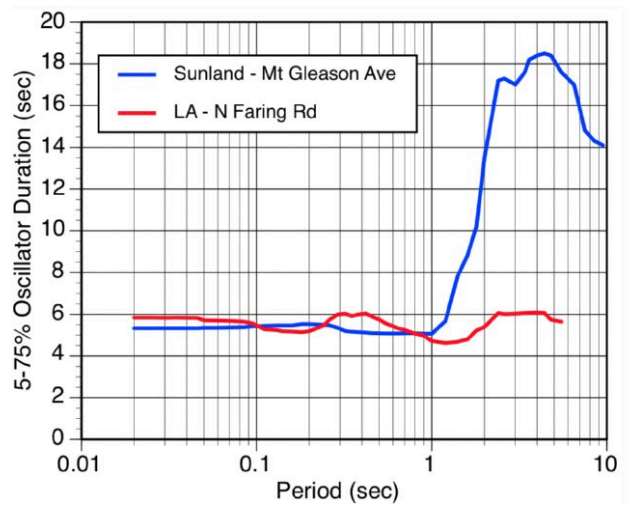


Figure 3. Example of recordings from the 1994 Northridge earthquake with similar acceleration (short-period) durations but very different long-period durations.

An alternative approach would be to bandpass filter the accelerograms and compute the duration of the AIN for the filtered accelerogram. A disadvantage of this approach is that for frequency bands with low amplitude, the filtered ground motion will tend to look like noise with durations that depend on the length of the recording. Using the response of the SDOF provides the effect of bandpass filtering but also reflects the amplitudes. Another advantage is that at very short periods (T=0), the duration of the SDOF becomes equal to the acceleration duration. Using the SDOF response provides duration values at different spectral periods that fits with the spectral periods used for the amplitude of the ground motion based on the response spectrum.

Data Set

For the preliminary period-dependent model, we used the NGA-W1 data set for which the full set of time series were available to compute the period-dependent duration. We limited the selected data to M>5.5 and $V_{\rm S30}>200$ m/s. We are expanding the data set to include recent recordings from California earthquakes with M>6 in the CSMIP data set and global earthquakes with M>7. The preliminary model shown in this paper will be updated using the expanded data set for the final model to be submitted to SMIP by May 2025.

Conditional Model for Period-Dependent Duration

There are two main approaches to developing ground-motion models (GMMs): (1) the traditional approach based on independent parameters such as magnitude, distance, and site condition and (2) the conditional GMM approach that includes a measure of the ground motion as an input parameter (Macedo et al., 2022). We use the conditional model for period-dependent duration for earthquakes in active crustal regions with the traditional D₅₋₇₅ duration acceleration duration (i.e., the duration for T=0 sec) used as an input parameter. The general form of the conditional GMM for the median period-dependent duration is given by:

$$D_{5-75}(T) = f_1(M, R, V_{S30}) + f_2(D_{5-75-acc})$$
(3)

in which the $D_{5-75-acc}$ is traditional duration of the accelerogram and the $f_1(M,R,V_{S30})$ term reflects the differences in the magnitude, distance, and site scaling for the $D_{5-75-acc}$ and the $D_{5-75}(T)$. A preliminary analysis showed that the magnitude dependent of $f_1(M,R,V_{S30})$ was not significant. That is, the magnitude scaling for the period-dependent duration is captured in the magnitude scaling of the $D_{5-75-acc}$ values. Therefore, we only included the distance and V_{S30} dependence in f_1 .

For duration, the source, path, and site effects are additive, not multiplicative as for response spectral values (Pinilla-- et al., 2024). We used a power-normal transformation for the duration, consistent with the Pinilla-Ramos et al. (2024) duration model for the acceleration duration. The functional for the conditional model is given by:

$$(D_{5-X}(T))^n = \left(c_1 + f_R(R_{RUP}) + c_4 \ln\left(\frac{v_{S30}}{500}\right) + c_5 D_{5-X,ACC}\right)^n + \delta \tag{4}$$

$$f_R = c_3 \ln(R_{RUP} + 1) + c_7 R_{RUP}$$

in which R_{RUP} is the rupture distance in km, V_{S30} is the time-averaged shear-wave velocity over the top 30 m in m/s, and $D_{5-X,ACC}$ is the significant duration measured from the accelerogram in sec. The δ are the residuals in units of sec and are assumed to be normally distributed with mean 0 and standard deviation σ .

The period dependence of the unsmoothed coefficients from the regression for D₅₋₇₅ and D₅₋₉₅ are shown in Figures 4 and 5, respectively. For both D₅₋₇₅ and D₅₋₉₅, the significant period dependence starts for T>0.5 sec. The c₅ is between 0.9 and 1.0 for T<4 sec indicating that the $D_{5-X}(T)$ has similar scaling with magnitude, distance, and site condition as the traditional $D_{5-X,ACC}$ metric. Comparing the coefficients for D₅₋₇₅ and D₅₋₉₅, the distance scaling is stronger for the D₅₋₉₅, whereas the V_{S30} scaling is stronger for the D₅₋₇₅. indicating that the effects of scattering in the crust along the ray path are more important for the duration from 75% to 95% part of the seismogram than for the 5-75% part.

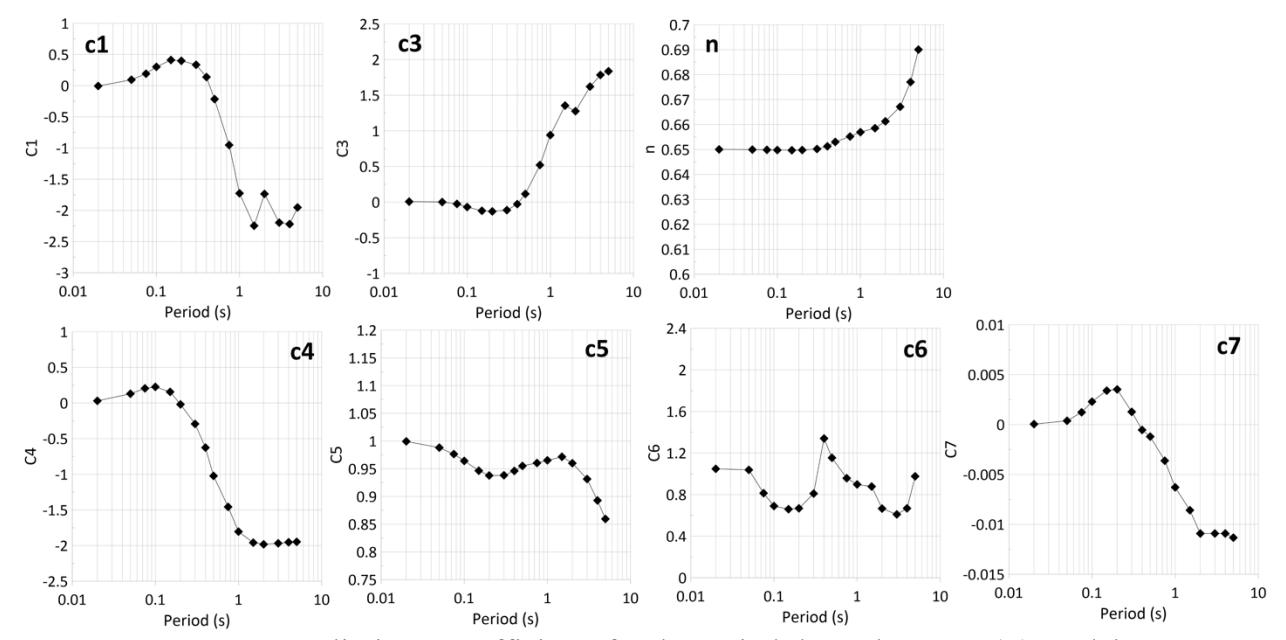


Figure 4. Preliminary coefficients for the period-dependent D₅₋₇₅(T) model.

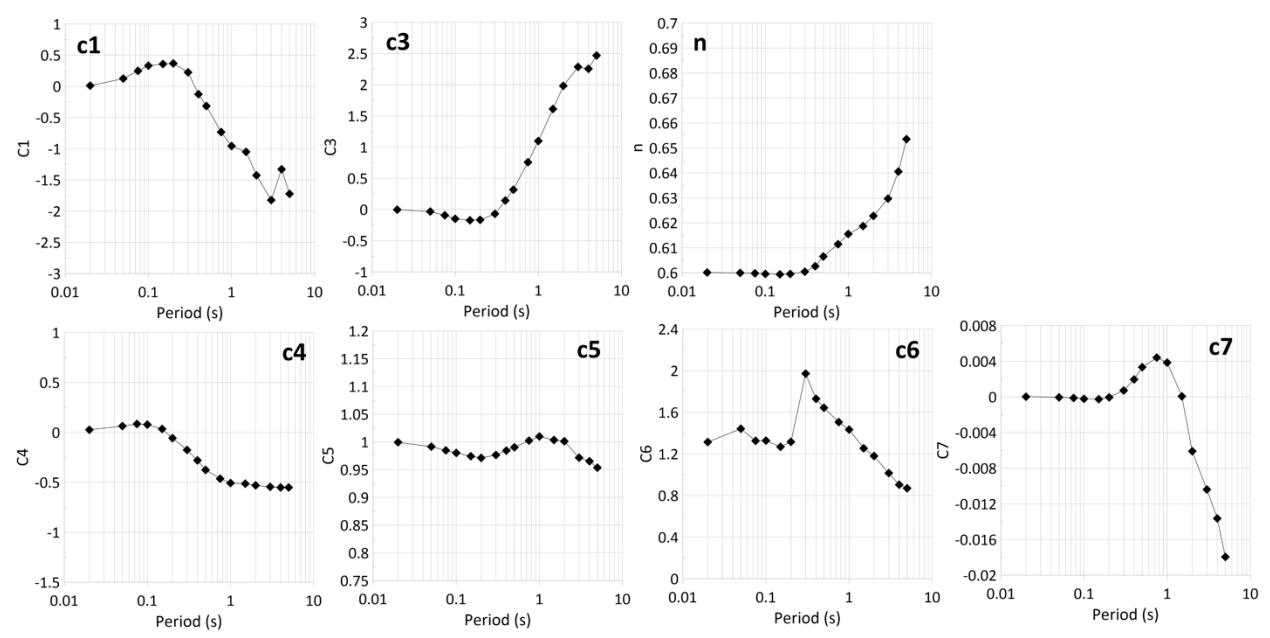


Figure 5. Preliminary coefficients for the period-dependent D₅₋₉₅(T) model.

Scaling of the Normalized Period-Dependent Duration

An example of the distance scaling of the $D_{5-75}(T)/D_{5-75-ACC}$ and $D_{5-95}(T)/D_{5-95-ACC}$ ratios are shown in Figure 6 for M=7 and V_{830} =400 m/s. The strongest distance dependence of the ratio is in the 1 to 10 km range. At distance beyond 10 km, the ratio has a weak distance dependence. The $D_{5-75}(T)/D_{5-75-ACC}$ ratio is near unity for all periods at 3 km distance whereas for the $D_{5-95}(T)/D_{5-95-ACC}$ ratio is near unity for all periods at about 1 km distance. At distances less than 1 km, the $D_{5-75}(T)/D_{5-75-ACC}$ ratio is less than unity at long periods, indicating that the long-period energy tends to be packed into a pulse at this very short distance.

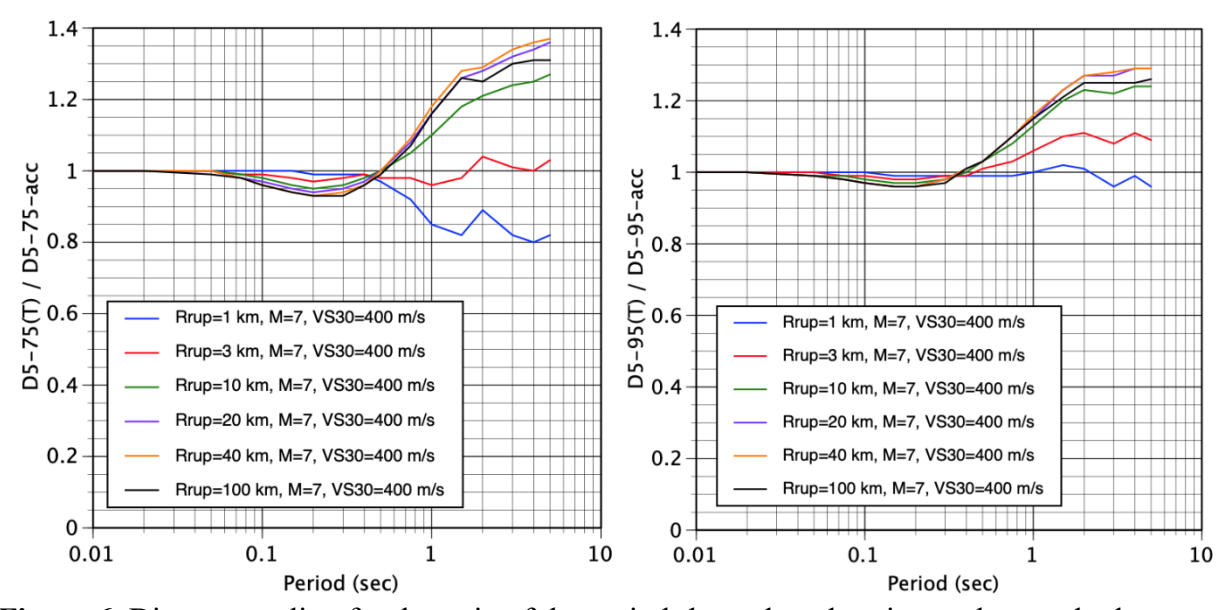


Figure 6. Distance scaling for the ratio of the period-dependent duration to the standard acceleration duration for the preliminary model without smoothing over period.

An example of the V_{S30} scaling of the $D_{5-75}(T)/D_{5-75-ACC}$ and $D_{5-95}(T)/D_{5-95-ACC}$ ratios are shown in Figure 7 for M=7 and R_{RUP} =10 km. For the $D_{5-75}(T)/D_{5-75-ACC}$ ratio, there is strong V_{S30} scaling with larger ratios for the softer sites, but for the $D_{5-95}(T)/D_{5-95-ACC}$ ratio, there is almost no V_{S30} dependence. This indicates that the contribution from the 75-95% range in the $D_{5-95}(T)$ is more affected by the scattering along the ray path than by the site effect on the duration.

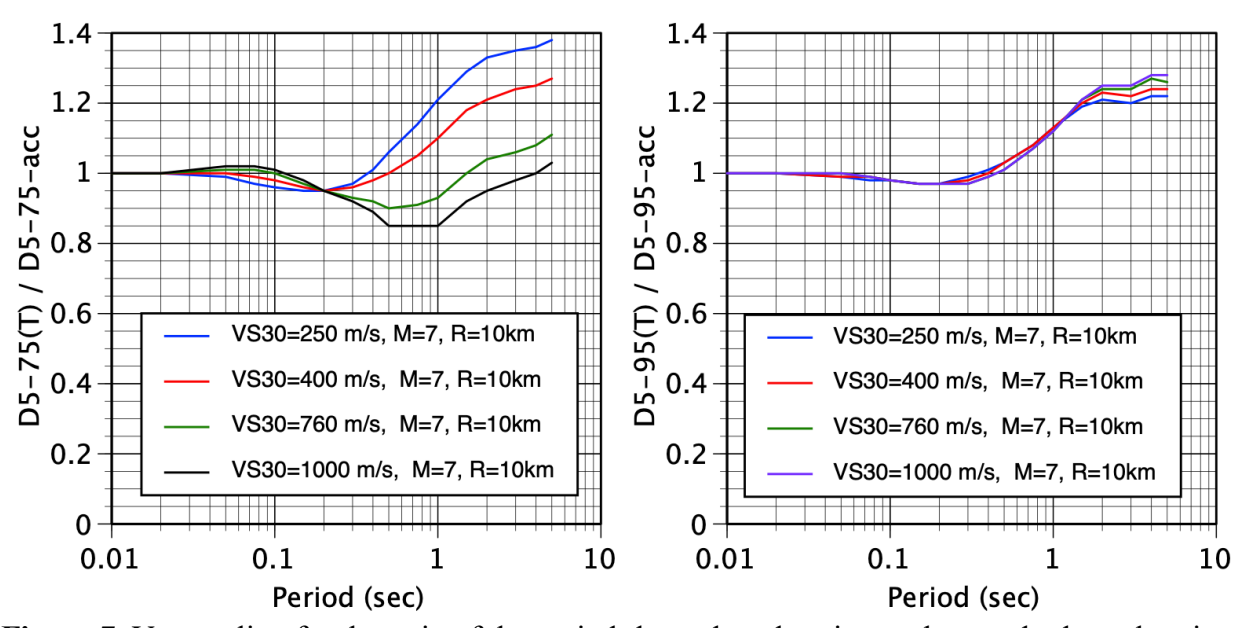


Figure 7. $V_{\rm S30}$ scaling for the ratio of the period-dependent duration to the standard acceleration duration for the preliminary model for M=7 and $R_{\rm RUP}$ =10 km.

Scaling of the Period-Dependent Duration

An example of the distance scaling of the unnormalized $D_{5-75}(T)$ and $D_{5-95}(T)$ are shown in Figure 8 for M=7 and V_{S30} =400 m/s. The strong distance scaling at short periods reflects the duration scaling in the reference $D_{5-75-ACC}$ model. At the long periods (T>1 sec), the distance scaling of the $D_{5-75}(T)$ and $D_{5-95}(T)$ becomes stronger than at short periods due to the distance scaling of the $D_{5-75}(T)/D_{5-75-ACC}$ and $D_{5-75}(T)/D_{5-75-ACC}$ ratios.

An example of the $V_{\rm S30}$ scaling of the unnormalized $D_{5\text{-}75}(T)$ and $D_{5\text{-}95}(T)$ are shown in Figure 9 for M=7 and $R_{\rm RUP}$ =10 km. For the $D_{5\text{-}75}(T)$ model, the $V_{\rm S30}$ scaling at short periods weak, indicating the weak dependence on $V_{\rm S30}$ in the reference $D_{5\text{-}75\text{-}ACC}$ model. At long periods (T>0.5 sec), the $D_{5\text{-}75}(T)$ ahs stronger $V_{\rm S30}$ scaling indicating a key difference in the duration scaling for short and long periods. For the $D_{5\text{-}95}(T)$ model, the $V_{\rm S30}$ scaling is similar at short and long periods due to the weak $V_{\rm S30}$ scaling in the $D_{5\text{-}95}(T)/D_{5\text{-}95\text{-}ACC}$ ratio.

An example of the magnitude scaling of the unnormalized D₅₋₇₅(T) and D₅₋₉₅(T) are shown in Figure 10 for R_{RUP} =15 km and and V_{S30} =400 m/s. There is no magnitude scaling in the D₅₋₇₅(T)/D_{5-75-ACC} and D₅₋₉₅(T)/D_{5-95-ACC} ratios, so the magnitude scaling is the same for short and long periods. The duration model is additive (constant shift on a linear scale) which gives the appearance of a change when plotted on a log scale.

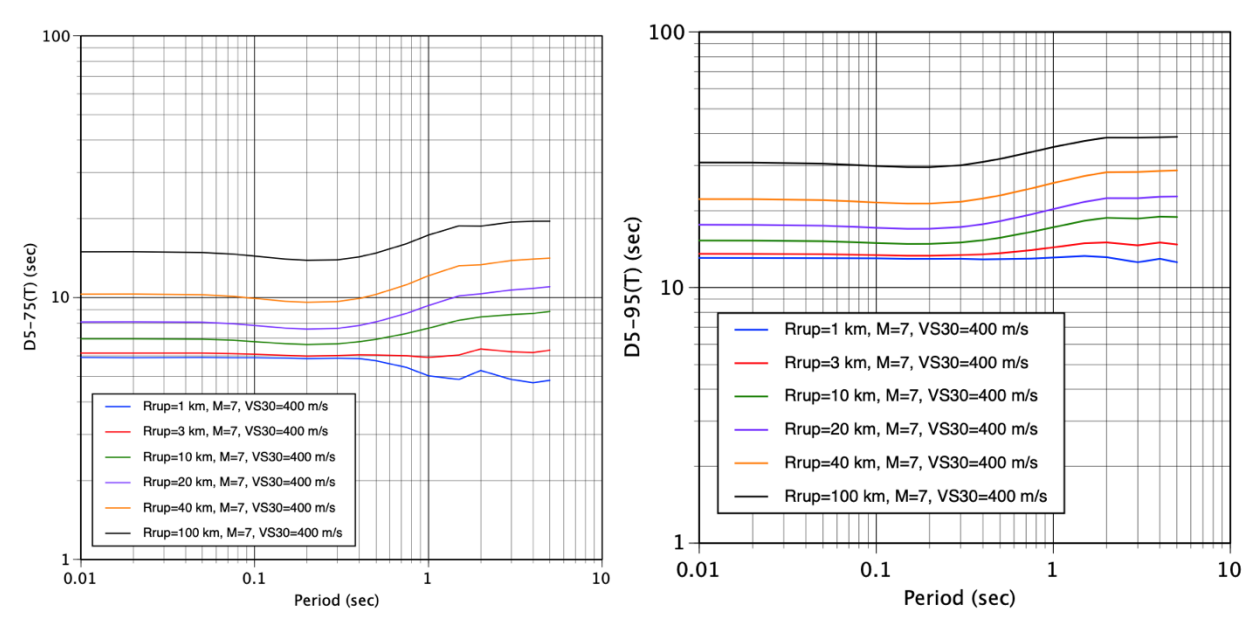


Figure 8. Example of the distance scaling for the period-dependent duration for the preliminary model for M=7 and $V_{\rm S30}$ =400 m/s.

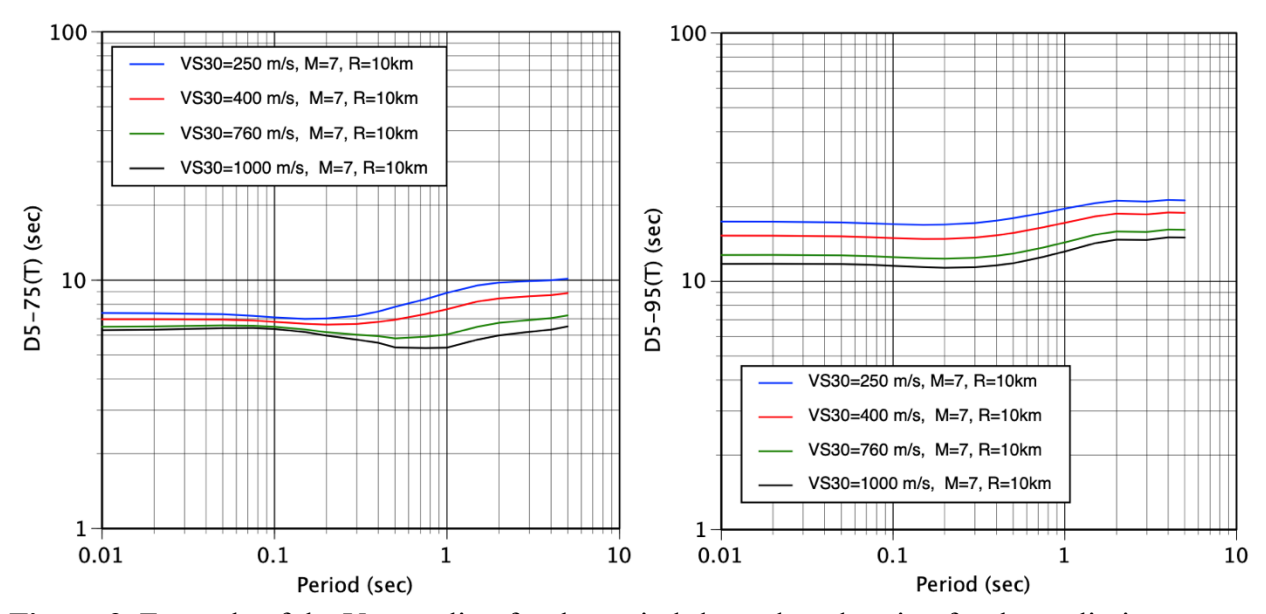


Figure 9. Example of the $V_{\rm S30}$ scaling for the period-dependent duration for the preliminary model for M=7 and $R_{\rm RUP}$ =10 km.

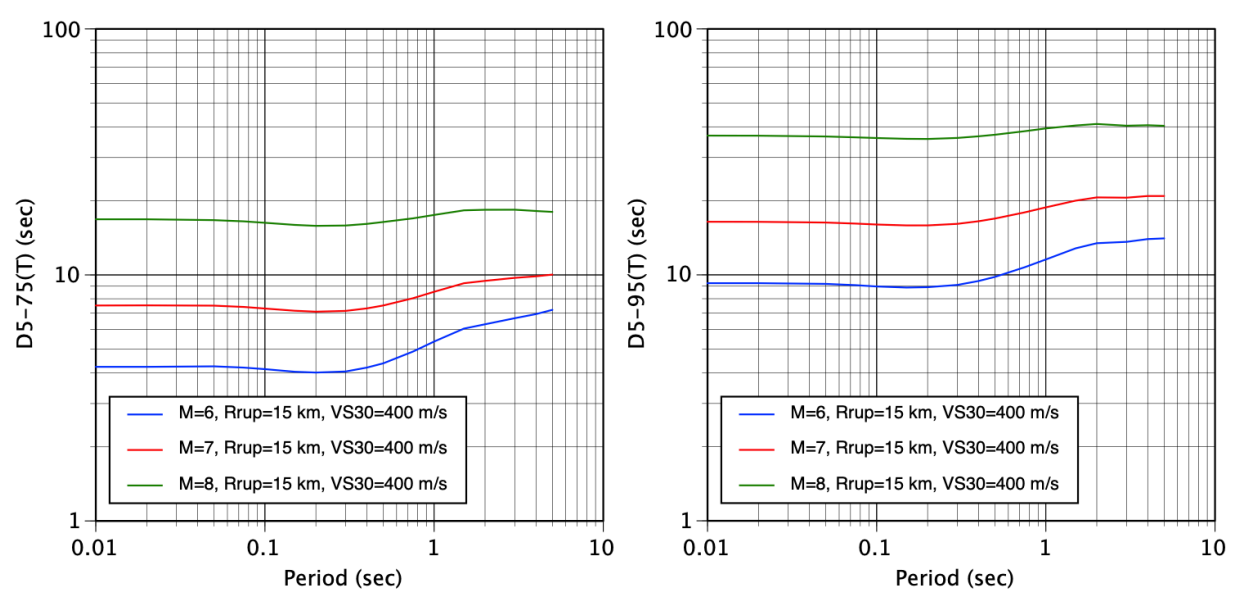


Figure 10. Example of the magnitude scaling for the period-dependent duration for the preliminary model for $R_{RUP}=15$ km and $V_{S30}=400$ m/s.

Example Application

As an example application of the period-dependent duration model, we consider a scenario with M=7, strike-slip, R_{RUP}=15 km, and V_{S30}=270 m/s. The response spectrum is computed for thee 84th percentile ground motion (left frame in Figure 11). Given this scenario and response spectrum, the period-dependent duration is computed by first computing the traditional D_{5-75-acc} and D_{5-95-acc} values using the Pinilla-Ramos et al. (2024) duration model. The Pinilla-Ramos et al. (2024) model includes the negative correlation between the epsilon at the PGA and the duration. The D_{5-75-acc} and D_{5-95-acc} values are then used as inputs to the conditional period-dependent duration models to compute the D₅₋₇₅(T) and D₅₋₉₅(T). The resulting 16th, median, and 84th percentile values for the duration spectra for D₅₋₇₅(T) and D₅₋₉₅(T) are shown in the center and left frames of Figure 11. These duration spectra can be used to set the target range of the duration for the development of time histories for inputs to the dynamic analyses of the structure. Using this target range for the period-dependent duration will help to avoid selecting time histories with long-period durations that are not centered on the target range.

Conclusions and Next Steps

The duration from the acceleration time series is not a good check on the duration of time histories for long-period structures. The period-dependent duration model can be used to develop design spectra for the duration that complement the standard design response spectra design. This will allow selection of ground motions with appropriate durations for dynamic analyses of long-period structures. This may lead to more consistent conclusions about the effect of duration on the structural response

Another use of duration is converting Fourier Amplitude Spectra (FAS) ground-motion models to response spectra models using RVT. In current applications, the amplitude has

assumed that ground motion duration is the same for all spectral periods (Kottke et al., 2021; Phung and Abrahamson, 2023). Using a period-dependent duration of the ground motion may improve the accuracy in converting FAS to response spectra.

Based on our initial results and feedback from SMIP, the next steps for the completion of the model are given below:

- (1) Complete the development and QA of the expanded data set.
- (2) Update the regression using the expanded data set
- (3) Extend the long-period range to 20 sec if the data are reliable up to 20 sec
- (4) Provide a computer program to compute the period-dependent duration from an accelerogram

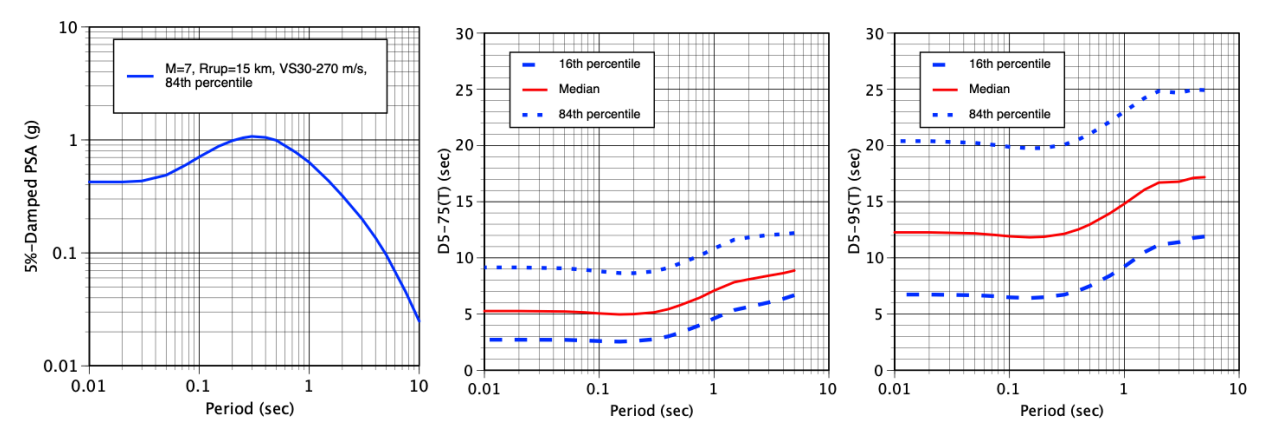


Figure 11. Example of the 84th percentile response spectrum for a scenario (M=7, Strike-slip, $R_{RUP}=15$ km, $V_{S30}=270$ m/s) and the corresponding duration spectra for the D_{5-75} and D_{5-95} duration. The duration spectra provide the target range of the period-dependent duration conditioned on this 84th percentile response spectrum and the M, R_{RUP} , and V_{S30} for this scenario.

References

Afshari, K. and J. Stewart (2016). Physically Parameterized Prediction Equations for Significant Duration in Active Crustal Regions, *Earthquake Spectra* Vol 32(4): 2057–2081.

Ancheta, T., R. Darragh, J. Stewart, E. Seyhan, W. Silva, B. Chiou, K. Wooddell, R. Graves, A. Kottke, D. M. Boore, T. Kishida, and J. Donahue (2014). NGA-West2 database, *Earthquake Spectra* Vol 30(3): 989–1005.

Arias, A. (1970). A measure of earthquake intensity, Seismic Design for Nuclear Power Plant - Cambridge, MA: MIT Press, 438–483.

Bommer, J. J. and A. Martínez-Pereira (1999). The Effective Duration of Earthquake Strong Motion. *Journal of Earthquake Engineering*, Vol 3(2): 127–172.

Bommer, J.J., P. J. Stafford, and J.E. Alarcón (2009). Empirical Equations for the Prediction of the Significant, Bracketed, and Uniform Duration of Earthquake Ground Motion, *Bull. Seismol. Soc. Am.*, 2009, Vol 99(6): 3217–3233.

Boore, D. and E. Thompson (2014). Path Durations for Use in the Stochastic-Method Simulation 276 of Ground Motions, *Bull. Seismol. Soc. Am.*, Vol 104(5): 2541–2552.

Du, W. and G. Wang (2017). Prediction equations for ground-motion significant durations using the NGA-West2 Database, *Bull. Seismol. Soc. Am.* Vol 107(1): 319–333.

- Hancock, J. and J. Bommer. (2006). A State-of-Knowledge Review of the Influence of Strong-Motion Duration on Structural Damage. *Earthquake Spectra*. Vol 22(3): 827–845.
- Kottke, A., N. Abrahamson, D. Boore, Y. Bozorgnia, C. Goulet, J. Hollenback, T. Kishida, O. Ktenidou, E. Rathje, W. Silva, E. Thompson, and X. Wang, (2021). Selection of random vibration theory procedures for the NGA-East project and ground-motion modeling, *Earthquake Spectra*, July 2021, Vol 37(1 suppl): 1420–1439.
- Macedo, J., C. Liu, and N. Abrahamson (2022). On the interpretation of conditional ground-motion models, *Bull. Seismol. Soc. Am.*, Vol. 112(5), pp. 2580-2586.
- Phung, V-B. and N. Abrahamson (2023). Conditional Ground-Motion Model Based on RVT Spectral Moments for Converting Fourier Amplitude Spectra to Response Spectra, *Bull Earthquake Eng*, Vol. 21: 5175–5207.
- Pinilla-Ramos, C., N. Abrahamson, V-B Phung, R. Kayan, and P. Castellanos-Nash (2024). Ground-motion model for significant duration constrained by seismological simulations, *Bull. Seismol. Soc. Am.*, Vol. 114 (2): 1015–1032
- Travasarou, T. (2003). Optimal ground motion intensity measures for probabilistic assessment of seismic slopes displacements, PhD Dissertation, University of California, Berkeley.